Precision predictions for future CEvNS experiments

XVIth Quark Confinement and the Hadron Spectrum
Cairns, Australia, August 2024

Jayden Newstead

Based on arXiv:2405.20060

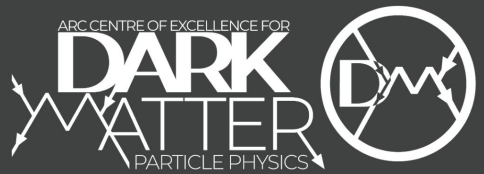

Collaborators:
Raghda Abdel Khaleq (ANU)
Cedric Simenel (ANU)
Andrew Stuchbery (ANU)

One-plot takeaway

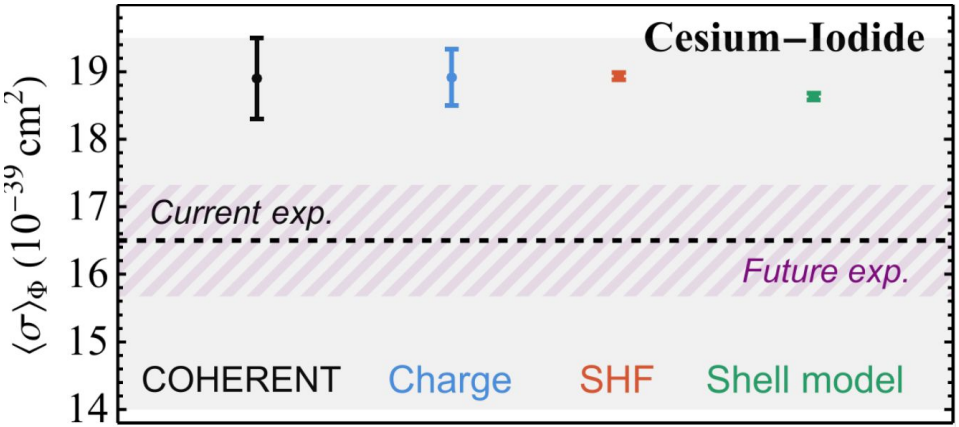

CEvNS introduction

Coherent
Elastic
ν (neutrino)
Nucleus
Scattering

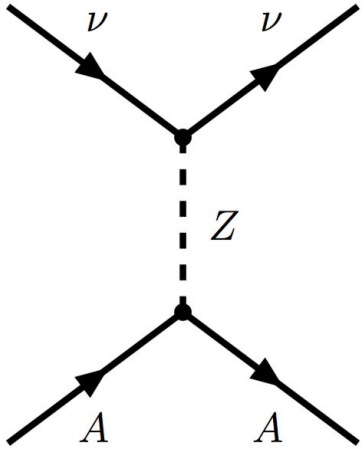

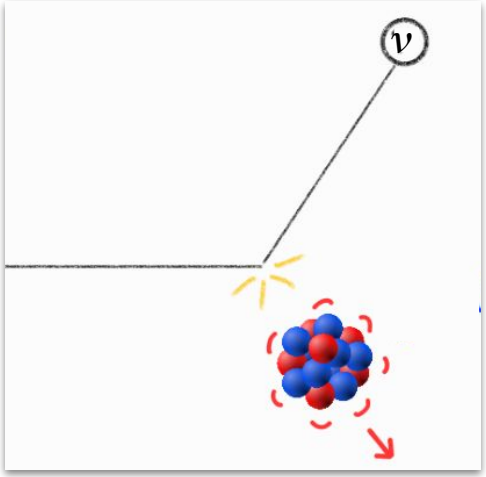

- Theorised: 1974 (Freedman)
- Observed: 2017 (COHERENT)

$$\frac{\mathrm{d}\sigma}{\mathrm{d}E_r}(E_r, E_\nu) = \frac{G_F^2}{4\pi} Q_W^2 m_N \left(1 - \frac{m_N E_r}{2E_\nu^2}\right) F^2(E_r)$$

$$Q_W = \mathcal{N} - (1 - 4\sin^2\theta_W)\mathcal{Z}$$

Motivations for CEvNS

- Tests of nuclear structure
- Reactor/waste monitoring
- New physics:
  - Modified nu couplings
  - Sterile neutrinos
  - Dark matter
- “Calibrate” background for dark matter experiments

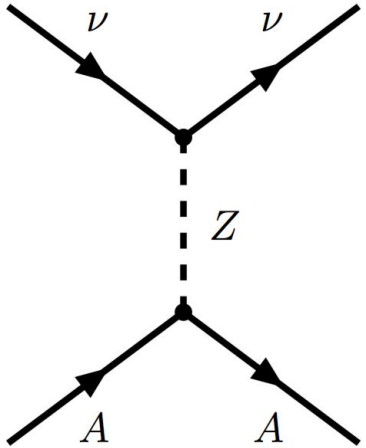

Detecting CEvNS

- Low-energy nuclear recoils
- Detected via scintillation, ionization, or phonons

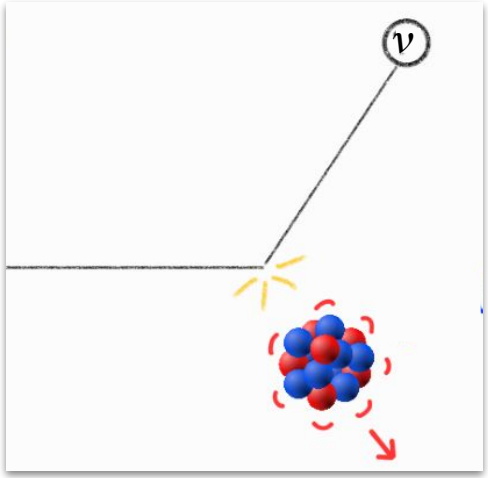

$E_{R,max}$: 10 eV 1 keV 100 keV

argon

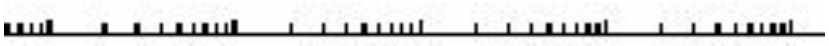

$E_{R,max}$: 10 eV 1 keV 100 keV

cesium

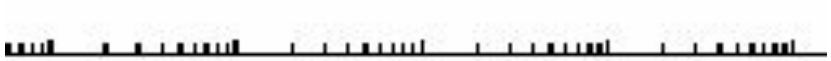

$$E_{R,\max} = \frac{2E_\nu^2}{m_T + 2E_\nu}$$

E_ν: 1 MeV 10 MeV 100 MeV

CEvNS experiments (an incomplete list)

Experiment	Source	Detector	Status
COHERENT	Stopped pion (SNS)	CsI, LAr, NaI, Ge	Running
CCM	Stopped pion (Lujan)	LAr	Running
CONNIE	Reactor (Argentina)	Si (Skipper CCD)	Running
CONUS+	Reactor (Switzerland)	HPGe	Running
MINER	Reactor (USA)	Ge, Si, Sapphire (cryo)	Building
NEON	Reactor (S. Korea)	NaI	Running
NUCLEUS	Reactor (France)	CaWO4 (cryogenic)	Building
RICOCHET	Reactor (France)	Ge (cryogenic) and Zn	Running
TEXONO	Reactor (Taiwan)	Ge (point contact)	Running
RELICS	Reactor (china)	Xe (TPC)	Building

Low-energy proton beam-dumps

Spallation sources:

SNS, ORNL (USA)
ISIS, RAL (UK)
Lujan, LANL (USA)
ESS (Sweden, *future*)

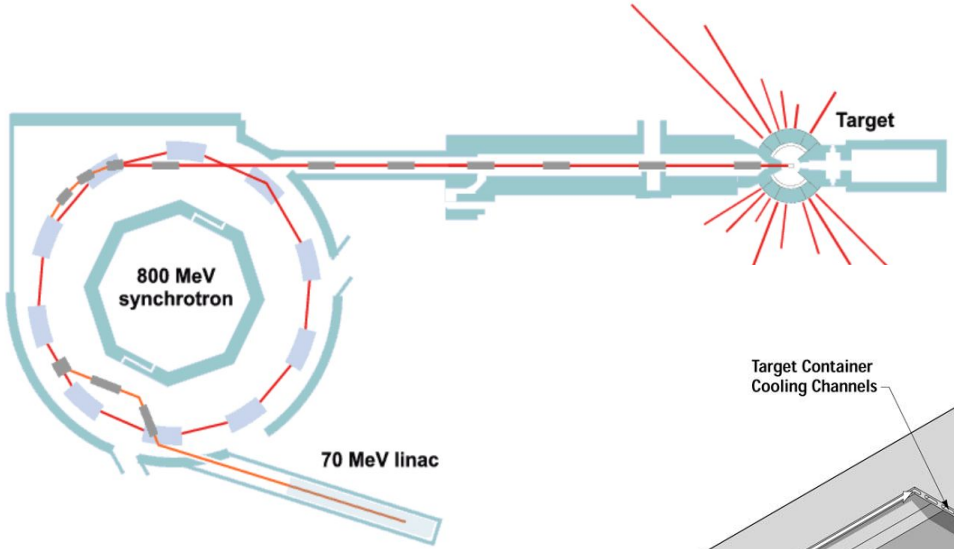

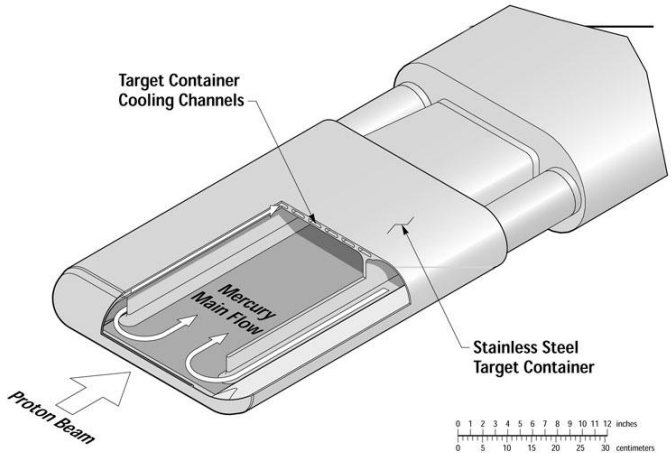

Credit: Bernie Riemer

Neutrino production

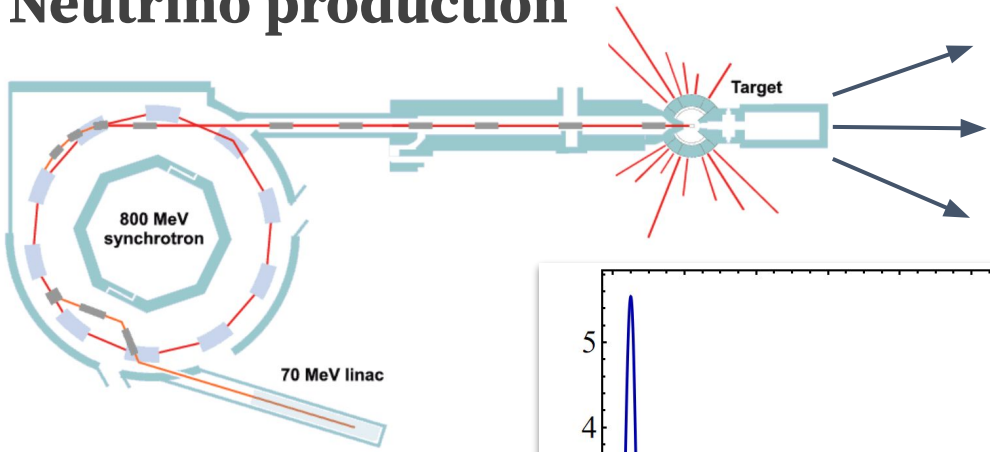

π^+ stopped

π^0 decays

π^- absorbed

$$\pi^+ \rightarrow \mu^+ + \nu_\mu$$
$$\downarrow$$
$$e^+ + \nu_e + \bar{\nu}_\mu$$

SNS
Pulsed @ 60Hz
Flux ~ 10^5 ν_x/cm^2/s
(with 1.3 MW beam)

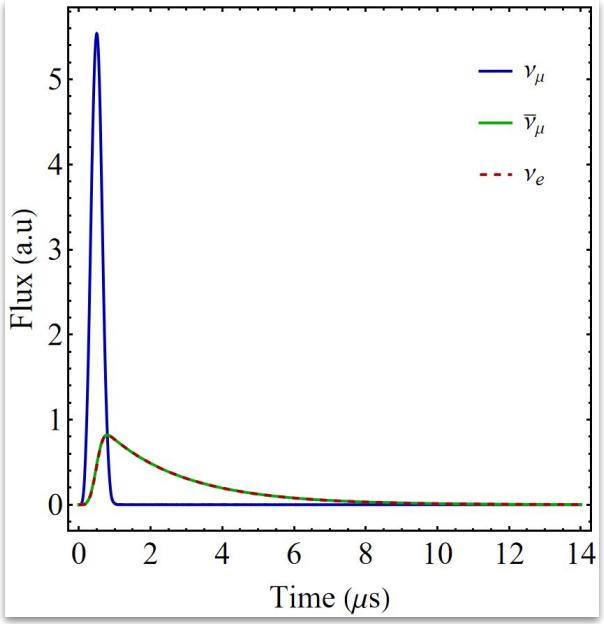

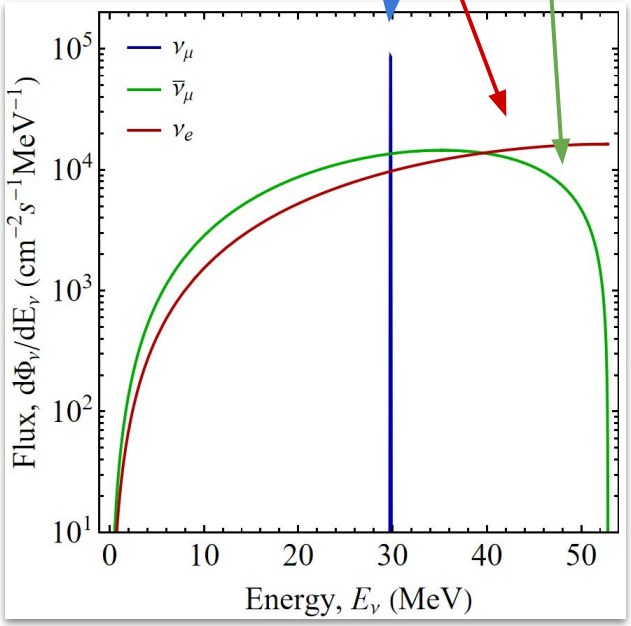

Detecting neutrinos at beam dumps

Lower threshold → Higher threshold

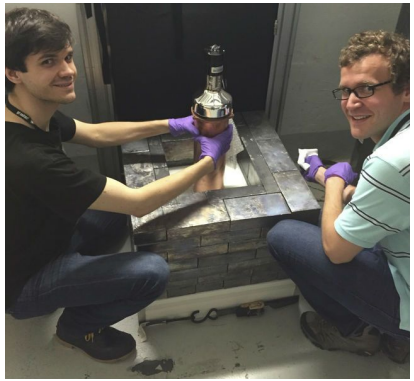

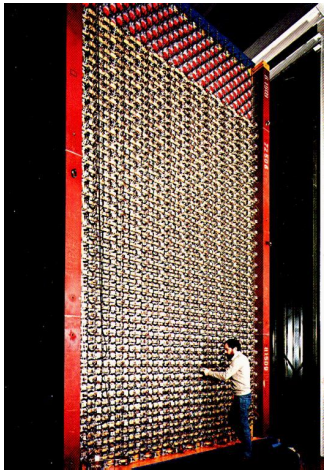

	COHERENT (SNS)	**CCM** (Lujan)	**KARMEN** (ISIS)
Target:	CsI	argon	organic scintillator (carbon)
Mass:	14.6 kg	10 t	56 t

Detecting neutrinos at beam dumps

- Neutrinos can be detected via neutral current (elastic or inelastic) or charged current interactions

Elastic scattering nuclear recoil (~keV):

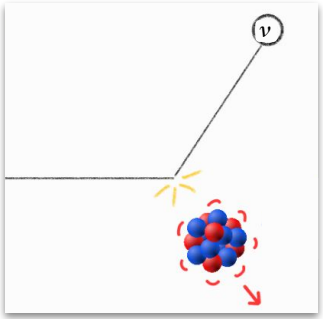

$$E_{R,\max} = \frac{2E_\nu^2}{m_T + 2E_\nu^2} = 50 \text{ keV}$$

$\sigma = 2 \times 10^{-38} \text{cm}^2$ at 30 MeV (cesium)

Pro: large σ
Con: hard to detect, larger backgrounds

NC inelastic scattering deexcitation (~MeV):

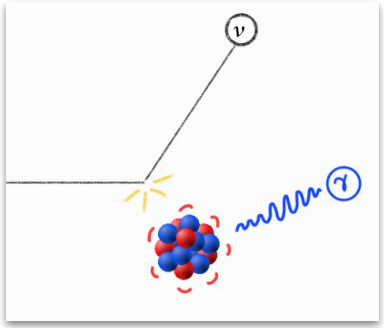

$$\omega_{\max} \approx E_\nu \left(1 - \frac{E_\nu^2}{2m_T^2}\right)$$

$^{12}\text{C}(\nu, \nu')^{12}\text{C}^*(1^+, 1; 15.1 \text{ MeV})$

$\sigma = 3 \times 10^{-42} \text{cm}^2$ at 30 MeV

Pro: easier to detect, line search lower bg
Con: smaller σ, larger theoretical uncertainties

Detecting neutrinos at beamdumps

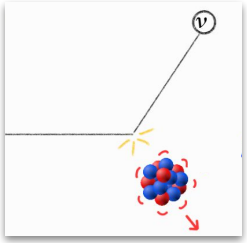

- The elastic scattering channel is known as CEvNS, was first observed in 2017 by COHERENT

Elastic (CEvNS) cross section:

$$\frac{\mathrm{d}\sigma}{\mathrm{d}E_r}(E_r, E_\nu) = \frac{G_F^2}{4\pi} Q_W^2 m_N \left(1 - \frac{m_N E_r}{2E_\nu^2}\right) F^2(E_r)$$

Where the weak charge is:

$$Q_W = \mathcal{N} - (1 - 4\sin^2\theta_W)\mathcal{Z}$$

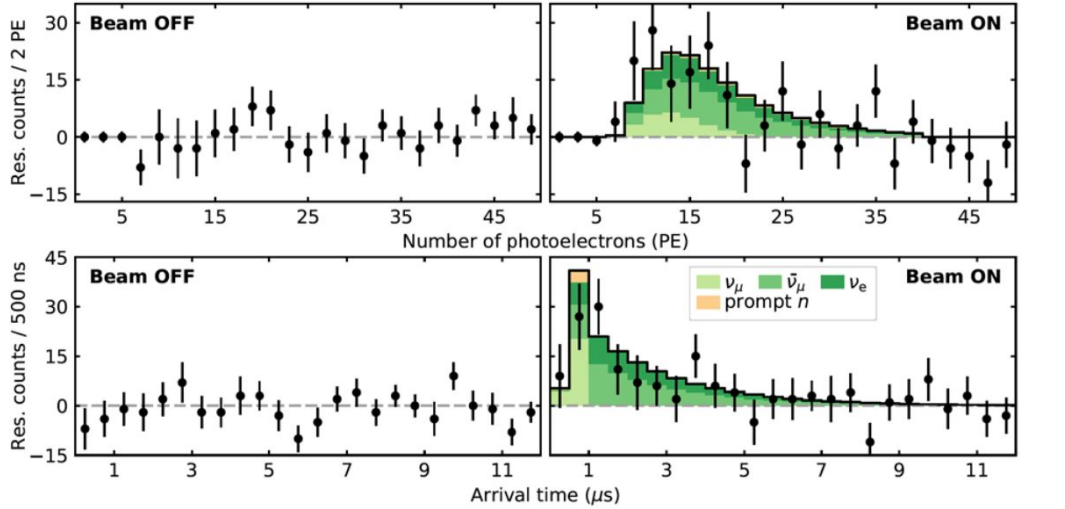

COHERENT Collaboration arXiv:1708.01294

Other CEvNS observations?

CONUS (reactor):

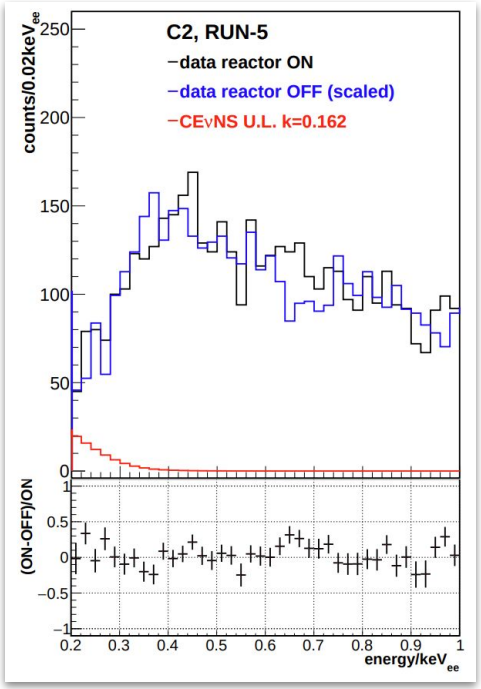

CONUS collaboration arXiv:2401.07684

XENONnT (boron-8):

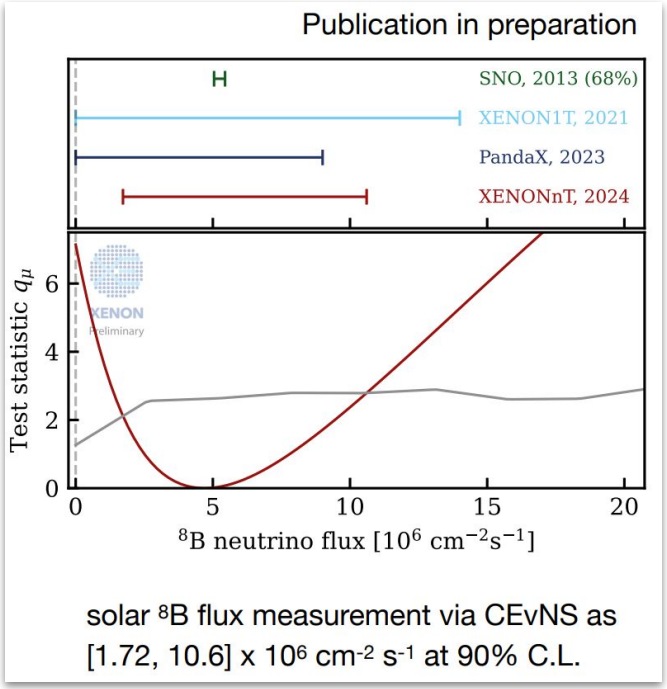

Fei Gao (XENON) [IDM2024](IDM2024)

Detecting neutrinos at beamdumps

- The COHERENT program includes multiple detectors in ‘neutrino alley’ at the SNS
- CEvNS with CsI, Ar, Ge targets (current)
- CC with D_2O

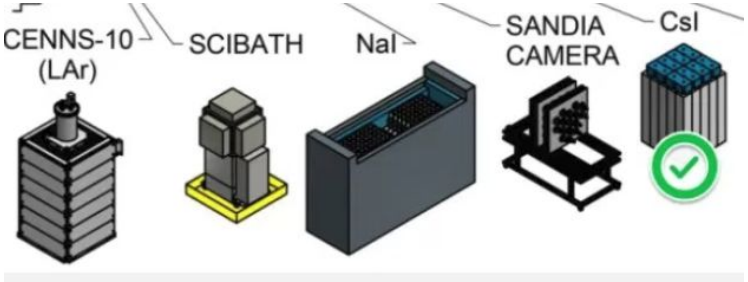

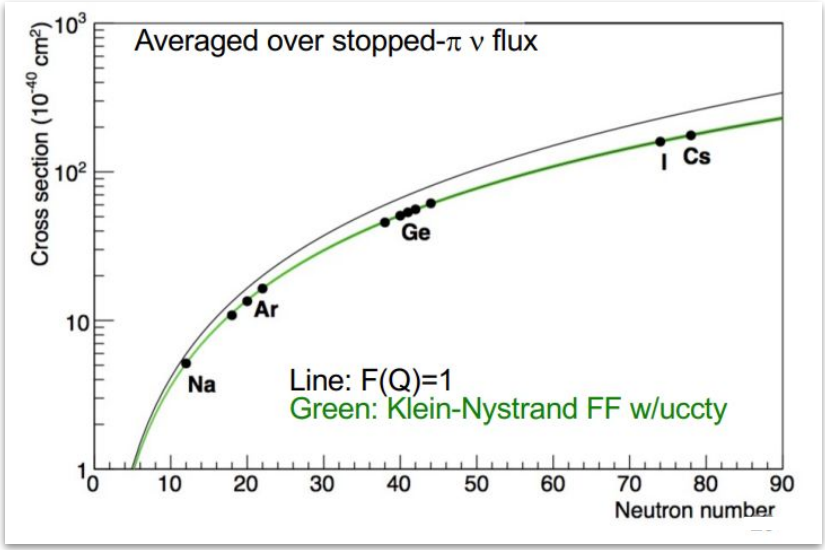

Credit: Kate Scholberg and the COHERENT Collaboration

Constraining new physics with COHERENT

- For example: non-standard neutrino-quark interactions (NSI)

NSI (model ind. Beyond SM):

SM weak charge is:

$$Q_W = \mathcal{N} - (1 - 4\sin^2\theta_W)\mathcal{Z}$$

$$Q_W^2 \equiv \Big[Z(g_p^V + 2\epsilon_{\alpha\alpha}^{uV} + \epsilon_{\alpha\alpha}^{d}) + N(g_n^V + \epsilon_{\alpha\alpha}^{uV} + 2\epsilon_{\alpha\alpha}^{d})\Big]^2$$

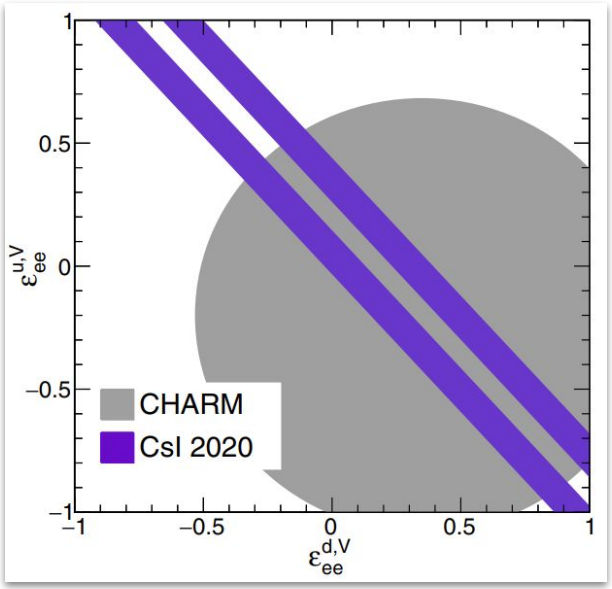

→ *Can also look for light mediators, steriles, dark matter…*

COHERENT Collaboration PRL (2022)

Revisiting the cross-section calculation

Complete coherent elastic neutrino-nucleus cross section

From Hofrichter, Menendez & Schwenk (PRD 2020):

$$\frac{d\sigma_A}{dE_R} = \frac{G_F^2 m_T}{4\pi}\left(1 - \frac{m_T E_R}{2E_\nu^2} - \frac{E_R}{E_\nu}\right) Q_{\mathrm{w}}^2 |F_{\mathrm{w}}(\mathbf{q}^2)|^2 + \frac{G_F^2 m_T}{4\pi}\left(1 + \frac{m_T E_R}{2E_\nu^2} - \frac{E_R}{E_\nu}\right) F_A(\mathbf{q}^2),$$

Weak form factor (M and **Φ**'' responses)

Axial form factor (**Σ**' response)

Weak nuclear charge

$$Q_{\mathrm{W}} = Q_{\mathrm{W}}^{p} Z + Q_{\mathrm{W}}^{n} (A - Z)$$

Flavor-dependent radiative corrections from *Tomalak et al. (JHEP 2021)*:

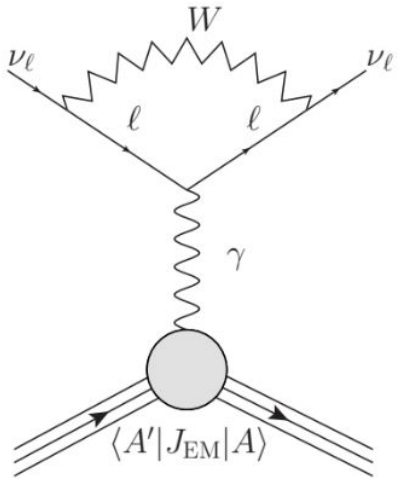

$$Q_{\mathrm{W}}^{n} = -1.02352(25)$$

$$Q_{\mathrm{W}}^{p,\nu_e} = 0.0747(34)$$

$$Q_{\mathrm{W}}^{\nu_e} - Q_{\mathrm{W}}^{\nu_\mu} = 0.01654Z$$

$$Q_{\mathrm{W}}^{\nu_\mu} - Q_{\mathrm{W}}^{\nu_\tau} = 0.00876Z$$

Nuclear form factors

$$
\begin{aligned}
F_{\rm w}(\mathbf{q}^2) = \frac{1}{Q_{\rm w}}\Bigg[&\left(Q_{\rm w}^p\left(1+\frac{\langle r_E^2\rangle^p}{6}t+\frac{1}{8m_N^2}t\right)\right.\\
&\left.+Q_{\rm w}^n\frac{\langle r_E^2\rangle^n+\langle r_{E,s}^2\rangle^N}{6}t\right)\mathcal{F}_p^M(\mathbf{q}^2)\\
&+\left(Q_{\rm w}^n\left(1+\frac{\langle r_E^2\rangle^p+\langle r_{E,s}^2\rangle^N}{6}t+\frac{1}{8m_N^2}t\right)\right.\\
&\left.+Q_{\rm w}^p\frac{\langle r_E^2\rangle^n}{6}t\right)\mathcal{F}_n^M(\mathbf{q}^2)\\
&-\frac{Q_{\rm w}^p(1+2\kappa^p)+2Q_{\rm w}^n(\kappa^n+\kappa_s^N)}{4m_N^2}t\mathcal{F}_p^{\Phi''}(\mathbf{q}^2)\\
&-\frac{Q_{\rm w}^n(1+2\kappa^p+2\kappa_s^N)+2Q_{\rm w}^p\kappa^n}{4m_N^2}t\mathcal{F}_n^{\Phi''}(\mathbf{q}^2)\Bigg]
\end{aligned}
$$

$$
\begin{aligned}
F_A(\mathbf{q}^2) &= \frac{8\pi}{2J+1}\\
&\times\left((g_A^{s,N})^2S_{00}^{\mathcal{T}}(\mathbf{q}^2)-g_Ag_A^{s,N}S_{01}^{\mathcal{T}}(\mathbf{q}^2)+(g_A)^2S_{11}^{\mathcal{T}}(\mathbf{q}^2)\right)\\
S_{00}^{\mathcal{T}} &= \sum_L\left[\mathcal{F}_+^{\Sigma'_L}(\mathbf{q}^2)\right]^2,\\
S_{11}^{\mathcal{T}} &= \sum_L\left[[1+\delta'(\mathbf{q}^2)]\mathcal{F}_-^{\Sigma'_L}(\mathbf{q}^2)\right]^2,\\
S_{01}^{\mathcal{T}} &= \sum_L 2\left[1+\delta'(\mathbf{q}^2)\right]\mathcal{F}_+^{\Sigma'_L}(\mathbf{q}^2)\mathcal{F}_-^{\Sigma'_L}(\mathbf{q}^2)
\end{aligned}
$$

Hofrichter, Menendez & Schwenk (PRD 2020)

Evaluating nuclear responses

We need:

$$|\mathcal{F}_N^X(q^2)|^2 \equiv \frac{4\pi}{2J_i+1} \sum_{J=0} \langle J_i||X_J^{(N)}||J_i\rangle\langle J_i||X_J^{(N)}||J_i\rangle,$$

$$|\mathcal{F}_N^{\Sigma'}(q^2)|^2 \equiv \sum_{J=1} \langle J_i||\Sigma_J'^{(N)}||J_i\rangle\langle J_i||\Sigma_J'^{(N)}||J_i\rangle,$$

For this we use the code DMformfactor (Fitzpatrick, Haxton, Anand)

Write the doubly reduced nuclear matrix elements in terms of single particle matrix elements:

$$\langle J_f; T_f \vdots\vdots \hat{O}_{J;T} \vdots\vdots J_i; T_i\rangle = \sum_{|\alpha|,|\beta|} \psi_{JT}^{f,i}(|\alpha|,|\beta|)\langle|\alpha|; \tfrac{1}{2}\vdots\vdots O_{J;T}\vdots\vdots|\beta|; \tfrac{1}{2}\rangle.$$

One body density matrix

Shell model & Skyrme-Hartree-Fock calculations

We used NuShellX with interactions:

Cs/I: SN100PN and GCN5082

Ar: SDPF-NR/U/MU and EPQQM

Ge: jj44b and JUN45

We used the SKYAX code with functionals:

SkM*
SLy6
SV-min
UNEDF1

- axial symmetry assumed2

Neutron skin: ~0.1 - 0.14 fm ~0.1 - 0.25 fm

See Abdel Khaleq et al. PRD 2024 and arXiv:2405.20060 for details

Weak form factors

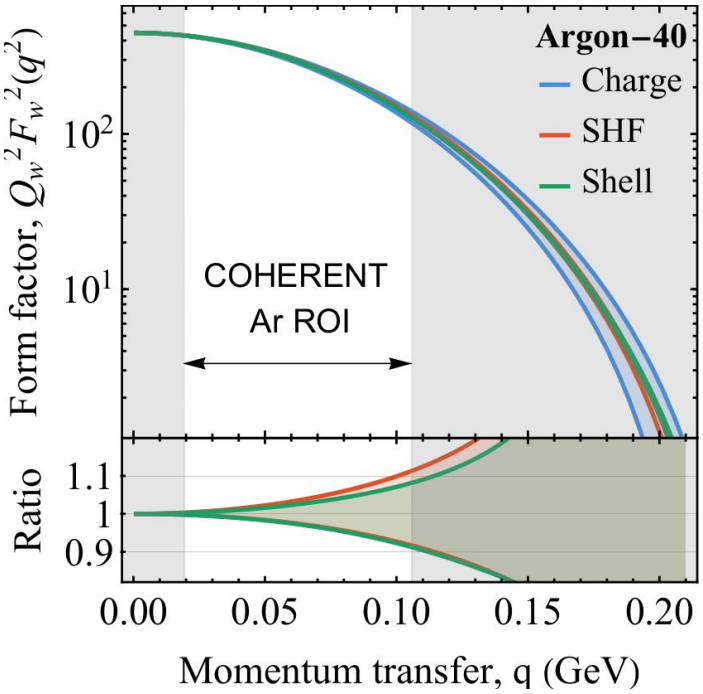

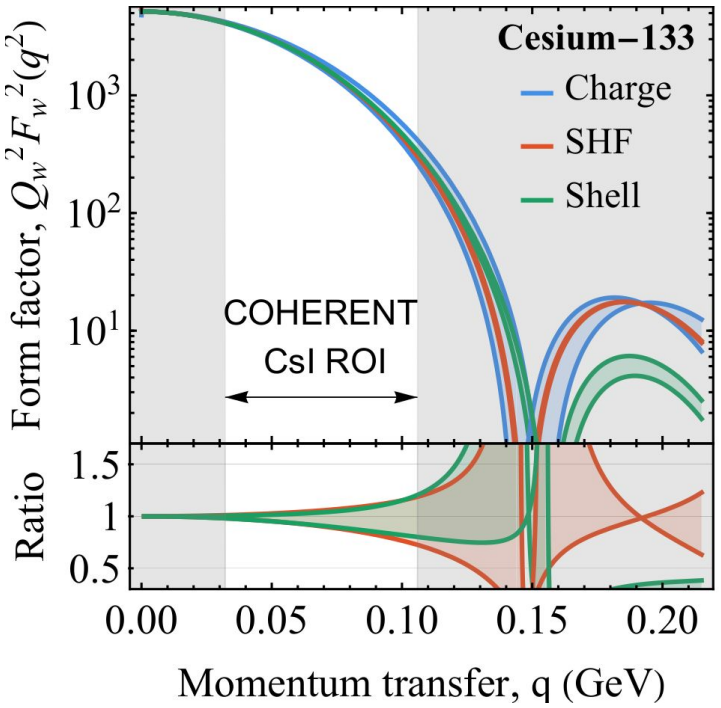

Spin form factors

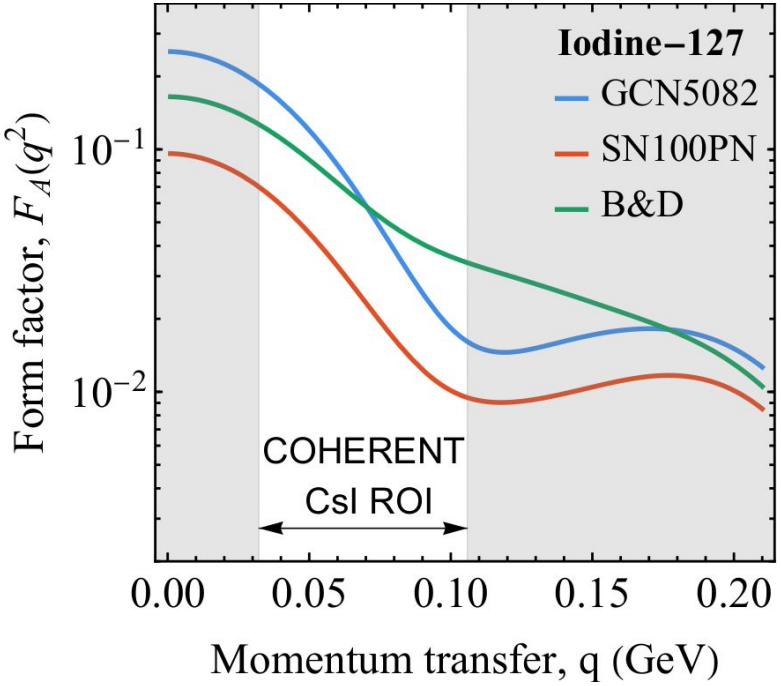

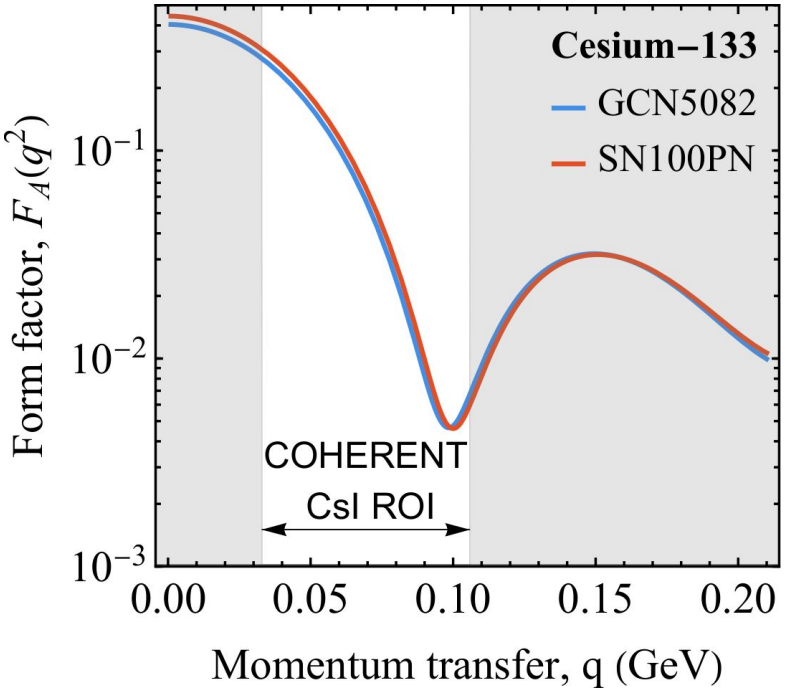

Cross section (from the shell model)

Cesium-133

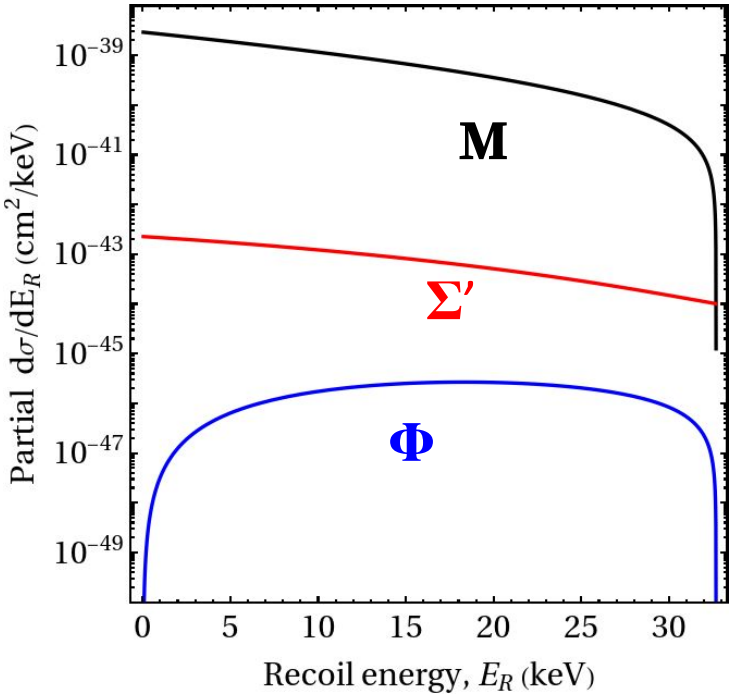

Argon-40

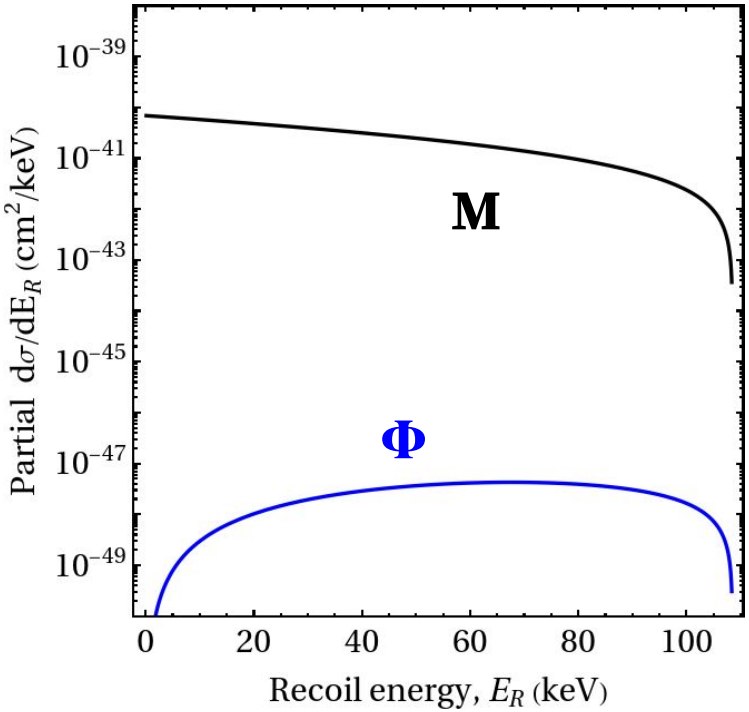

Nuclear operators beyond M have tiny contributions

Flux averaged cross sections

$$\langle\sigma\rangle_\Phi = \int dE_\nu \frac{d\phi}{dE_\nu} \int dE_R \frac{d\sigma}{dE_R}$$

				COHERENT	
Target	Charge	SHF	Shell Mod.	Prediction	Exp.
Ar	18.65(22)	18.68(6)	18.64(5)	18.0(4)	23(7)
Ge	59(1)	59.8(2)	59.2(2)	-	-
CsI	189(4)	189.3(5)	186.3(5)	189(6)	165(30)

CsI uncertainty 3.2% → 0.8%

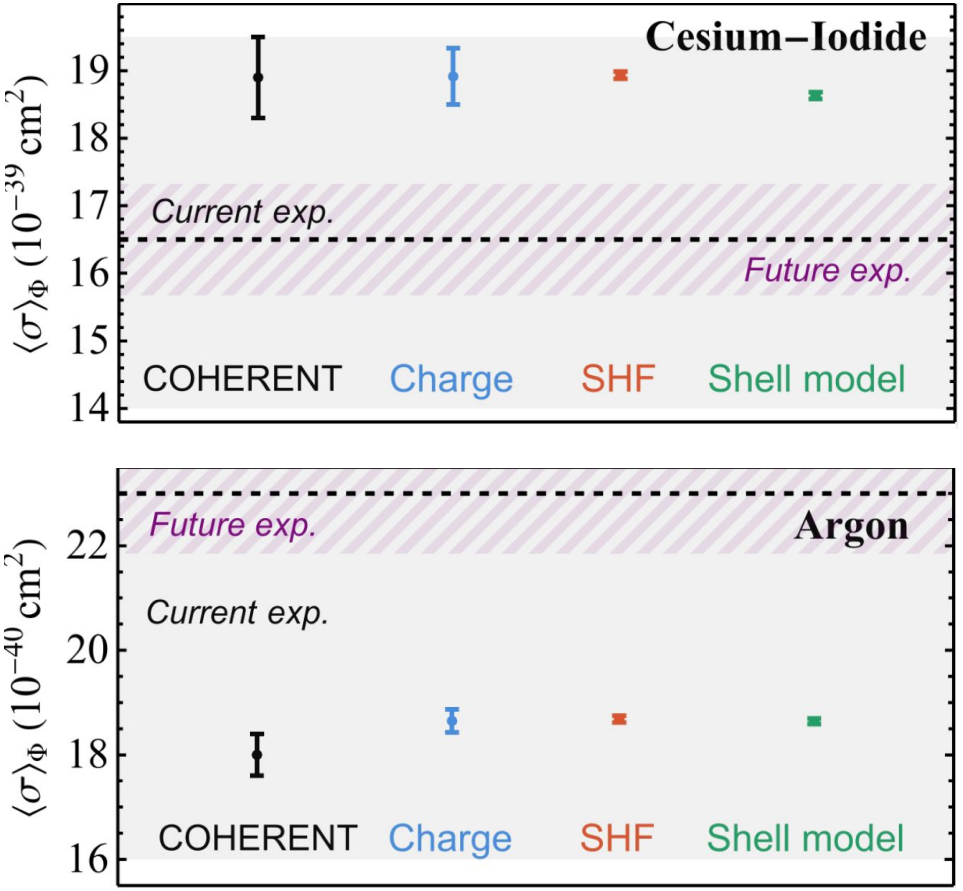

COHERENT event rates

$$N^{\mathrm{CsI}}_{\mathrm{events}} = N_T\,\Phi \int dPE\,\epsilon(PE) \times \int dE_R P(PE|E_R)\frac{dR}{dE_\nu}$$

$$N^{\mathrm{Ar}}_{\mathrm{events}} = N_T\,\Phi \int dE_{ee}\epsilon(E_{ee}) \times \int dE_R\,P(E_{ee}|E_R)\frac{dR}{dE_\nu}$$

Target	Mass	Distance	POT	$\langle\pi/\mathrm{POT}\rangle$
Ar	24.4 kg	27.5 m	1.38×10^{23}	0.09
CsI	14.6 kg	19.3 m	3.20×10^{23}	0.0848

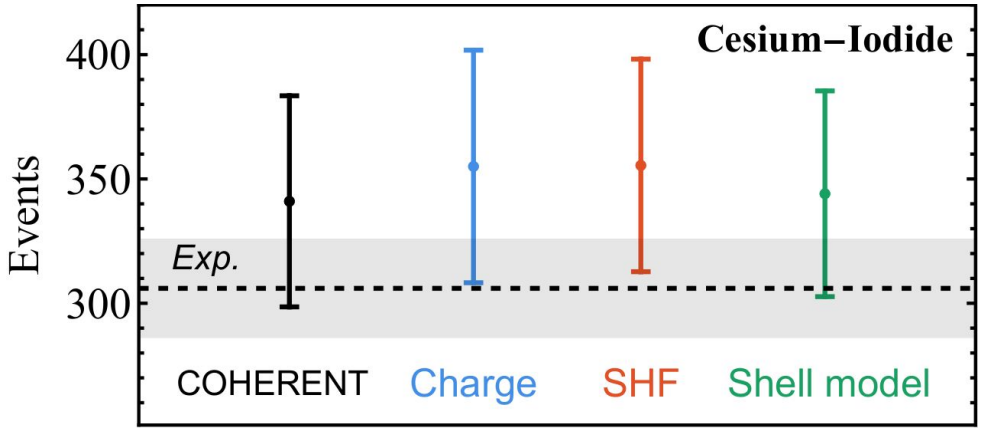

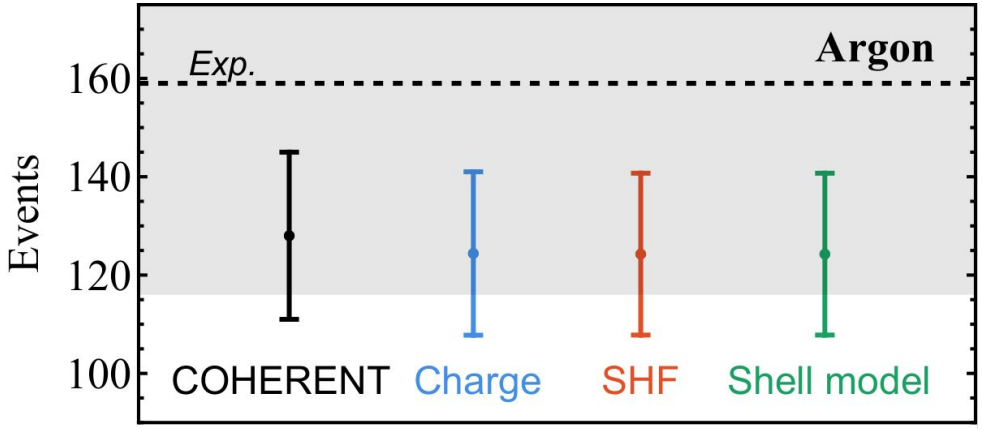

Summary

- Lots of CEvNS experiments are coming online
- High-statistics regime coming -> higher precision predictions desired
- We found axial and spin-orbit operators are very small ($< 10^{-4}$)
- SHF and shell model agree at <1% level
- Sub-percent precision achieved

"The universe drawn by Dali" by DALL.E

National Partners

International Partners

Weak radius results

SHF:

Nucleus	R_p (fm)	R_n (fm)	R_W (fm)
^{40}Ar	3.326(25)	3.420(17)	3.514(17)
^{70}Ge	3.930(21)	3.986(12)	4.065(12)
^{72}Ge	3.946(20)	4.036(12)	4.116(12)
^{73}Ge	3.954(19)	4.059(11)	4.140(12)
^{74}Ge	3.963(18)	4.084(10)	4.165(11)
^{76}Ge	3.993(20)	4.143(14)	4.224(15)
^{127}I	4.688(14)	4.824(9)	4.895(10)
^{133}Cs	4.750(12)	4.887(8)	4.957(9)

Shell model:

Nucleus	Interaction	R_p (fm)	R_n (fm)	R_w (fm)
^{40}Ar	SDPF-NR	3.32852	3.43528	3.53293
	SDPF-U	3.32852	3.43528	3.53282
	SDPF-MU	3.32851	3.43528	3.53243
	EPQQM	3.32851	3.43528	3.53348
^{70}Ge	GCN2850	3.95524	4.05401	4.13886
	JUN45	3.95843	4.05818	4.14331
	jj44b	3.95963	4.07061	4.15307
^{72}Ge	GCN2850	3.97233	4.07882	4.16942
	JUN45	3.97412	4.11049	4.19586
	jj44b	3.97457	4.12156	4.20457
^{73}Ge	GCN2850	3.97979	4.11144	4.20019
	JUN45	3.98047	4.13135	4.21644
	jj44b	3.97981	4.14185	4.22461
^{74}Ge	GCN2850	3.98664	4.14437	4.23118
	JUN45	3.98951	4.16453	4.24903
	jj44b	3.98955	4.17113	4.25434
^{76}Ge	GCN2850	4.00136	4.20041	4.28574
	JUN45	4.00456	4.21257	4.29678
	jj44b	4.00422	4.21636	4.29966
^{127}I	B&D	4.6651	4.89861	4.97959
	SN100PN	4.66554	4.92354	4.99969
	Trun. SN100PN	4.66559	4.92575	5.00184
	GCN5082	4.66544	4.91281	4.98982
	GCN5082*	4.66425	4.91304	4.98979
^{133}Cs	SN100PN	4.72559	4.99394	5.06814
	SN100PN*	4.7252	4.99335	5.06752
	GCN5082	4.72545	4.99188	5.06646
	GCN5082*	4.72493	4.99011	5.06455

Shell model model spaces